Hard X-ray Luminosity Function of Tidal Disruption Events: First Results from *MAXI* Extragalactic Survey

Taiki Kawamuro,[1] Yoshihiro Ueda,[1] Megumi Shidatsu,[2] Takafumi Hori,[1]
Nobuyuki Kawai,[3] Hitoshi Negoro,[4] and Tatehiro Mihara[2]

[1] Department of Astronomy, Kyoto University, Kyoto 606-8502, Japan
[2] *MAXI* team, RIKEN, 2-1, Hirosawa, Wako-shi, Saitama 351-0198, Japan
[3] Department of Physics, Faculty of Science Tokyo Institute of Technology, Tokyo 152-8551, Japan
[4] Department of Physics, Nihon University, 1-8-14 Kanda-Surugadai, Chiyoda-ku, Tokyo 101-8308, Japan
E-mail(TK): kawamuro@kusastro.kyoto-u.ac.jp

Abstract

We derive the first hard X-ray luminosity function (XLF) of stellar tidal disruption events (TDEs) by supermassive black holes (SMBHs), which gives an occurrence rate of TDEs per unit volume as a function of peak luminosity and redshift, utilizing an unbiased sample observed with the *MAXI*. On the basis of the light curves characterized by power-law decay with an index of $-5/3$, a systematic search using the *MAXI* data in the first 37 months detected four TDEs, all of which have been found in the literature. To formulate the TDE XLF, we consider the mass function of SMBHs, that of disrupted stars, the specific TDE rate as a function of SMBH mass, and the fraction of TDEs with relativistic jets. We perform an unbinned maximum likelihood fit to the *MAXI* TDE list. The results suggest that the intrinsic fraction of the jet-accompanying events is 0.0007%–34%. We confirm that at $z \lesssim 1.5$ the contamination by TDEs to the hard X-ray luminosity functions of active galactic nuclei is not significant and hence that their contribution to the growth of SMBHs is negligible at the redshifts.

Key words: galaxies: active — X-rays: galaxies

1. Introduction

Tidal disruption events (TDEs) by supermassive black holes (SMBHs) occur when a star gets close to a SMBH enough for the tidal force to exceed the self-gravity of the star. A part of the disrupted star subsequently accretes onto the SMBH, which is observed as a luminous flare. These suggest that the TDE contributes to the mass growth of SMBHs. To quantitatively discuss the effect of TDEs on the growth history, luminosity dependence of the TDE rate, or "luminosity function", has to be constrained based on a statistically complete sample.

Some studies have theoretically estimated the occurrence rate of TDEs to be 10^{-5}–10^{-4} galaxy^{-1} yr^{-1} (e.g., Magorrian & Tremaine 1999). Many observational results (e.g., Donley et al. 2002) are in rough agreements with the predicted TDE rate. Furthermore, the dependence of the rate on SMBH mass is numerically calculated (e.g., Stone & Metzger 2014). Considering that the flare luminosity of a TDE depends on the SMBH mass, it is possible theoretically to estimate the luminosity function of TDEs (Milosavljević et al. 2006). However, observational studies that directly constrain the TDE luminosity function based on a statistically complete sample have been limited so far.

X-ray surveys covering a large sky area are very useful to detect TDEs, and to make the complete sample, because we cannot predict when and where an event occurs. In fact, wide-area X-ray surveys performed with *ROSAT*, *XMM-Newton*, *INTEGRAL*, and *Swift* (e.g., Komossa & Bade 1999; Burrows et al. 2011; Nikołajuk & Walter 2013) have discovered many of the TDEs. Sometimes accompanying relativistic jets were reported. The identifications of TDEs were mainly based on their variability characteristics, such as a large amplitude and the unique decline law of the light curve (e.g., Komossa & Bade 1999).

In this proceeding, we present the derivation of the hard X-ray luminosity function (XLF) of TDEs, using a statistically complete sample. Based on the *MAXI* mission, we make the sample by systematically searching for hard X-ray transient events at high galactic latitudes ($|b| > 10^\circ$), and identify TDEs. We then derive the XLF of TDEs associated with and without relativistic jets individually. Eventually, the result enables us to estimate

the contribution of TDEs to the mass growth of SMBHs. Note that more details are presented in Kawamuro et al. (2016).

Throughout this proceeding, we assume a Λ cold dark-matter model with $H_0 = 70$ km s^{-1} Mpc^{-1}, $\Omega_{\rm M} = 0.3$, and $\Omega_\Lambda = 0.7$. The "log" denotes the base-10 logarithm, while the "ln", the natural logarithm.

2. Search of TDE From *MAXI* Data

2.1. Observations and Data Reduction

In this work, we search for TDEs by utilizing the *MAXI*/GSC data (Matsuoka et al. 2009; Mihara et al. 2011). The *MAXI*/GSC has two instantaneous fields-of-view of 1°.5×160° separated by 90 degrees. By rotating according to the orbital motion of the international space station, it covers a large fraction of the sky (95%) in one day (Sugizaki et al. 2011). We analyze the data taken in the first 37 months since the beginning of the operation (from 2009 September 23 to 2012 October 15). We also restrict our analysis to high galactic latitudes ($|b| > 10°$). Hence, the data we use are the same as those made for creating the second *MAXI*/GSC catalog (Hiroi et al. 2013), which contains 500 sources detected in the 4–10 keV band from the data integrated over the whole period. The details of the data selection criteria are described in Section 2 of Hiroi et al. (2013).

2.2. Identification of TDEs in *MAXI* Catalogs

To detect TDEs whose typical time scale of months to years (e.g., Komossa & Bade 1999) as completely as possible, we newly construct the *MAXI*/GSC "*transient source catalog*". We optimize the analysis to find variable objects on the time scale of 30 or 90 days. Namely, we split the whole data into 30 or 90 day bins, and independently perform source detection in each dataset to search for new sources that are not listed in the 2nd *MAXI* catalog (Hiroi et al. 2013). The detail can be found in Appendix 1 of Kawamuro et al. (2016). As a result, we detect 10 transient sources with the detection significance $s_{\rm D} > 5.5$ in either of the time-sliced datasets, where $s_{\rm D}$ is defined as (best-fit flux in 4–10 keV)/(its 1σ statistical error). The sensitivity limit for the peak flux averaged for 30 days is ~ 2.5 mCrab.

On the basis of positional coincidence, we identify 3 TDE candidates in the *MAXI* transient source catalog from the literature, *Swift* J1112.2–8238 (hereafter *Swift* J1112–82; Brown et al. 2015), *Swift* J1644+57 (Burrows et al. 2011), and *Swift* J2058.4+0516 (hereafter *Swift* J2058+05; Cenko et al. 2012). We also identify another candidate that occurred in NGC 4845 (Nikołajuk & Walter 2013), which has been already listed in the 2nd *MAXI*/GSC catalog (Hiroi et al. 2013). The detailed information of each TDE from the literature is summarized in Table 1.

Table 1. Our Sample of Tidal Disruption Events

Name	z	$\log L_{\rm X}$	Γ	δ	M_*
[1]	[2]	[3]	[4]	[5]	[6]
Swift J1112.2–8238	0.89	47.1	-	-	-
Swift J164449.3+573451	0.354	46.6	10	16	0.15
Swift J2058.4+0516	1.1853	47.5	> 2	-	0.1
NGC 4845	0.004110	42.3	-	-	0.02

Notes.
Col. [1]: Name of the TDE. Col. [2]: Redshift. Col. [3]: Luminosity (erg s^{-1}) in the 4–10 keV band. Col. [4]: The Bulk Lorentz factor. Col. [5]: The Doppler factor. Col. [6]: Accreted mass in units of solar mass.

2.3. Search for Unidentified TDEs

To derive the XLF, it is very important to perform a complete survey at a given flux limit. Hence, we search for other possible TDEs that are not reported in the literature from these *MAXI* catalogs. We make use of the general characteristics of the light curve pattern of TDEs: rapid flux increase and power-law decay with an index of –5/3 as a function of time (Phinney 1989). For this purpose, we make the light curves of all sources in the 2nd *MAXI*/GSC catalog (Hiroi et al. 2013) and in the transient catalog in 10 days, 30 days, and 90 days bins, in three energy bands, 3–4 keV, 4–10 keV, and 3–10 keV. The fluxes in each time bin are obtained by the same image fitting method as described in Appendix 1 of Kawamuro et al. (2016).

As the reference, we analyze the light-curve of the four identified TDEs and find that all of them satisfy the following two characteristics. The first one is high variability amplitudes: the ratio between the highest flux and the one of the previous bin in the 30-day (90-day) averaged light curves is above 5. The second one is that the decay light curves are consistent with a power-law profile of $t^{-5/3}$, where t is time since the onset time of each TDE. We note that the time of the flux peak, $t_{\rm p}$, is delayed from the TDE onset time by approximately 5–80 days. Hence, we set the central day of the bin showing the highest flux as $t_{\rm p}$, and estimate the TDE onset time by correcting for these offsets. A power-law fit to the light curve over 90 days after the peak flux is found to be acceptable in terms of a χ^2 test (Figure 1).

Accordingly, we apply the above two conditions to the light curves of all *MAXI* sources (in total 506) except for the four TDEs. As a result, we find that none of them satisfy the two criteria except for the objects identified as active galactic nuclei (AGNs) or X-ray galactic sources. Thus, we conclude that *MAXI* detected only the four TDEs identified above during the first 37 months of its operation. This sample can be regarded as a statistically complete one at the sensitivity limit of *MAXI* for transient events, as long as TDEs share similar characteristics in the X-ray light curve to those of the known

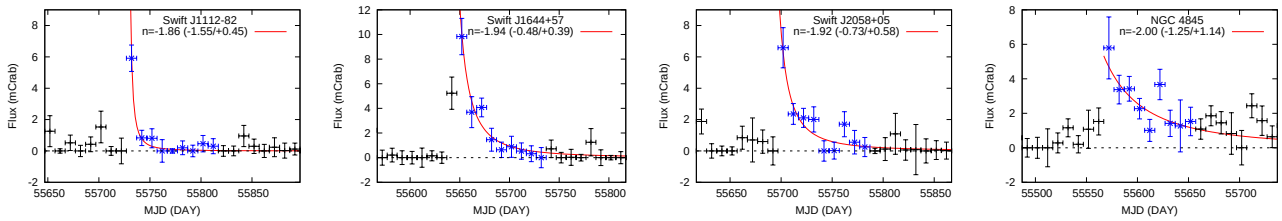

Fig. 1. X-ray (3–10 keV) light curves of four TDEs during their flares. Only blue regions are used to be fit with a power-law decay model. The best-fit power-law index (n) is indicated in each panel with errors at 90% confidence level.

events.

3. Hard X-ray Luminosity Function of Tidal Disruption Events

3.1. Definition of Luminosities

In this section, we summarize the definitions of TDE luminosities used in our analysis ($L_{\rm X}^{\rm obs}$ and $L_{\rm X}$). To make luminosity conversion between different energy bands, we need to assume model spectra of TDEs. According to the previous studies on TDEs observed in the X-ray band we can approximate that the X-ray spectra of TDEs without jets are composed of blackbody radiation and a power law, which originate from the optically thick disk and its Comptonized component by hot corona, respectively. For TDEs with jets, a relativistically beamed power law is added to the above spectrum.

We define $L_{\rm X}$ as the "intrinsic" peak luminosity of the Comptonized power-law component in the rest-frame 4–10 keV band. It can be converted into the "observed" peak luminosity by

$$L_{\rm X}^{\rm obs} = C L_{\rm X}, \tag{1}$$

where C (C_0 or C_1; see below) is the conversion factor that depends on the shape of the spectrum, redshift, and viewing angle with respect to the jet axis (for TDEs with jets).

Introducing the fraction of TDEs with jets in total TDEs, $f_{\rm jet}$, we divide TDEs into two types, one with jets and the other without jets. For the TDEs without jets, whose fraction is $(1-f_{\rm jet})$, the conversion factor C_0 can be written as

$$C_0 = \omega_{\rm pow} + \omega_{\rm bb}, \tag{2}$$

where $\omega_{\rm pow}$ and $\omega_{\rm bb}$ are those for the Comptonized (power-law) and blackbody components, respectively. We normalize $\omega_{\rm pow}$ to unity when $L_{\rm X}^{\rm obs}$ of a TDE at $z = 0$ is defined in the 4–10 keV band and its spectrum is not absorbed. The factor $\omega_{\rm bb}$ depends on the broadband spectrum of a TDE. Note that the blackbody component is negligible in the 4–10 keV band because its temperature is expected to be much lower than a few keV.

For TDEs with relativistic jets, the conversion factor C_1 can be written as

$$C_1 = \omega_{\rm pow} + \omega_{\rm bb} + \omega_{\rm jet}\eta_{\rm jet}\delta^4 \tag{3}$$

where the last term represents the jet contribution. Here, $\omega_{\rm jet}$ takes account of the energy-band conversion, and $\eta_{\rm jet}$ is the fraction of the intrinsic luminosity (i.e., that would be observed without beaming) of the jet in $L_{\rm X}$ (the peak luminosity of the Comptonized component). The Doppler factor (δ) is represented as

$$\delta = \frac{1}{\Gamma - \sqrt{\Gamma^2 - 1}\cos\theta}, \tag{4}$$

where Γ is the Lorentz factor and θ is the viewing angle with respect to the jet axis. The observed luminosity from the jet becomes larger than the intrinsic one by a factor of δ^4 with a frequency shift by δ. In our analysis, we adopt $\Gamma = 10$, which is suggested from the analysis of the spectral energy distribution of *Swift* J1644+57 by Burrows et al. (2011). We also adopt $\eta_{\rm jet} = 0.1$ as a standard value. The conversion factors C_0 and C_1 are dimensionless, composed only of the dimensionless factors (ω, $f_{\rm jet}$, and δ).

3.2. TDE Sample

We utilize the four identified TDEs listed in Table 1 as a complete sample from our *MAXI* survey, and derive the XLF. When integrated for 30 days, the *MAXI* survey covers all the high Galactic latitudes ($|b| > 10^\circ$) region, which corresponds to 83% of the entire sky. We have searched for TDEs based on 30 days or 90 days binned light curves. Thus, the sensitivity limit for the 30-days averaged peak flux of TDEs to which our survey is complete is determined by that for 30-days integrated data. The resultant limit is 2.5 mCrab, or 3×10^{-11} erg s^{-1} cm^{-2} (4–10 keV).

3.3. Formulation of TDE X-ray Luminosity Function

We define the XLF of TDEs so that $\mathrm{d}\Phi(L_{\rm X}, z)/\mathrm{d}L_{\rm X}$ represents the TDE occurrence rate per unit co-moving volume per $L_{\rm X}$ per unit rest-frame time, as a function of $L_{\rm X}$ and z, in units of Mpc^{-3} $L_{\rm X}^{-1}$ yr^{-1}.

In our work, we make simple assumptions for modelling the shape of the TDE XLF. First, we write the TDE occurrence rate per unit volume as a function of SMBH mass. It should be proportional to the product of the SMBH mass function (i.e., comoving number density of SMBHs) and a specific TDE rate in a single SMBH. The local SMBH mass function can be derived from the local luminosity function of galaxies and the Faber-Jackson relation between the galaxy luminosity and the SMBH mass ($L_{\rm gal} \propto M_{\rm BH}^k$) as

$$\psi(M_{\rm BH*}; M_{\rm BH}){\rm d}M_{\rm BH} = \psi_0 \Big(\frac{M_{\rm BH}}{M_{\rm BH*}}\Big)^{\gamma} e^{-(\frac{M_{\rm BH}}{M_{\rm BH*}})^k} \frac{{\rm d}M_{\rm BH}}{M_{\rm BH*}}. \quad (5)$$

Here, $\gamma = k(\alpha+1)-1$, where α is a parameter of the galaxy luminosity function defined as $\Psi(L_{\rm gal*}; L_{\rm gal}){\rm d}L = \Psi_0 (L_{\rm gal}/L_{\rm gal*})^{\alpha} e^{-L_{\rm gal}/L_{\rm gal*}} {\rm d}L_{\rm gal}/L_{\rm gal*}$. The subscript $*$ indicates the characteristic parameter. Unless otherwise noted, we adopt $k = 0.8$, $\Psi_0 = 0.007$, $\log(M_{\rm BH*}/M_\odot) = 8.4$, and $\alpha = -1.3$ according to the results obtained by Marconi & Hunt (2003) and Blanton et al. (2001), where $M_\odot$ is the solar mass. We refer to the dependence of the specific TDE rate on SMBH mass derived by Stone & Metzger (2014),

$$\xi \propto M_{\rm BH}^{\lambda}, \quad (6)$$

where λ is chosen to be -0.4.

To represent the TDE occurrence rate as a function of luminosity, we further make an assumption that the peak luminosity L of a TDE (i.e., that free from the jet luminosity) is proportional to the SMBH mass, or equivalently, a constant fraction of the Eddington luminosity, $\lambda_{\rm Edd}$. Then, by converting $M_{\rm BH}$ into L in the product of $\psi(M_{\rm BH*}; M_{\rm BH})$ and ξ, we can express the occurrence rate of TDEs per unit volume in terms of L as

$$\phi(L_*; L){\rm d}L = \psi_0 \xi_0 \Big(\frac{L}{L_*}\Big)^{\gamma+\lambda} e^{-(\frac{L}{L_*})^k} \frac{{\rm d}L}{L_*}. \quad (7)$$

We incorporate a redshift dependence of the TDE XLF with an evolution factor of $(1+z)^p$ that is multiplied to the local XLF. Thus, the TDE XLF is formulated as

$$\frac{{\rm d}\Phi(L_{\rm X}, z)}{{\rm d}L_{\rm X}} {\rm d}L_{\rm X} = (1+z)^p \phi(L_{\rm X*}; L_{\rm X}){\rm d}L_{\rm X}. \quad (8)$$

3.4. Mass Function of Stars Disrupted by SMBHs

A TDE occurs only when the tidal disruption radius, $R_{\rm TDE} = R_*(M_{\rm BH}/M_*)^{1/3}$, where M_* and R_* are the mass and radius of the star, is larger than the Schwarzschild radius, $R_{\rm Sch}$ ($\equiv 2GM_{\rm BH}/c^2$, where G and c is the gravitational constant and the light speed, respectively.). For a given star, there is an upper boundary for the mass of a SMBH that can cause a TDE. Hence, the mass function of stars should be incorporated in calculating the actual TDE XLF. We approximate it by the shape of an initial mass function (IMF) with an upper star mass boundary $M_{*,\rm max}$, considering that very massive stars are already dead due to their short life time. Here we employ the IMF derived by Kroupa (2001).

3.5. Maximum Likelihood Fit

We adopt the unbinned maximum likelihood (ML) method to constrain the XLF parameters. Whereas the ML fit gives the best-fit parameters, the goodness of the fit cannot be evaluated. Hence, we perform one dimensional Kolmogorov-Smirnov test (hereafter KS test) separately for the redshift distribution and for the luminosity distribution between the observed data and best-fit model. The p-value, the chance of getting observed data set, is evaluated from the one-sided KS test statistic.

We define the likelihood function as

$$\mathcal{L} = -2\sum_i \ln \frac{\int\int\int N(L_{\rm X}, L_{{\rm X}i}^{\rm obs}, z_i, M_*, \theta){\rm d}L_{\rm X}\,{\rm d}\log M_*\,{\rm d}\Omega/2\pi}{\int\int\int\int\int N(L_{\rm X}, L_{\rm X}^{\rm obs}, z, M_*, \theta){\rm d}L_{\rm X}{\rm d}L_{\rm X}^{\rm obs}{\rm d}z{\rm d}\log M_*{\rm d}\Omega/2\pi}, \quad (9)$$

where the subscript index i refers to each TDE and the denominator represents the number of observable TDEs with the intrinsic peak luminosity $L_{\rm X}$, the observed one $L_{\rm X}^{\rm obs}$, the redshift z, the mass of the star M_*, and the viewing angle θ, expected from the survey (note that θ is related to the solid angle as ${\rm d}\Omega = 2\pi{\rm d}(\cos(\theta))$). By considering that the fraction of TDEs with jets among all TDEs is $f_{\rm jet}$, the differential number is calculated as

$$\begin{aligned} &N(L_{\rm X}, L_{\rm X}^{\rm obs}, z, \theta, M_*) \\ &\quad = \Big\{(1-f_{\rm jet})\delta_{\rm D}(C_0 L_{\rm X} - L_{\rm X}^{\rm obs}) + f_{\rm jet}\delta_{\rm D}\Big(C_1 L_{\rm X} - L_{\rm X}^{\rm obs}\Big)\Big\} \\ &\quad \times \frac{{\rm d}\Phi(L_{\rm X}, z)}{{\rm d}L_{\rm X}} \frac{d_{\rm L}^2(z)}{1+z} c\frac{{\rm d}\tau}{{\rm d}z} A\Big(\frac{L_{\rm X}^{\rm obs}}{d_{\rm L}^2}\Big) \frac{\Delta T}{1+z} P(M_*), \end{aligned} \quad (10)$$

where $\delta_{\rm D}(x)$ is the Dirac δ-function, $d_{\rm L}$ the luminosity distance, ${\rm d}\tau/{\rm d}z$ the differential look-back time, A the survey area at the flux limit of $L_{\rm X}^{\rm obs}/4\pi d_{\rm L}^2$, and ΔT (= 37 months) the survey time at the observer's frame. The factor $1/(1+z)$ comes from the time dilation at z.

Since our sample size of TDEs is very small (four), we fix the following parameters of the XLF model, which cannot be well constrained from the data. We adopt the characteristic luminosity of $\log L_{\rm X*} = 44.6$ corresponding to the Eddington ratio of $\lambda_{\rm Edd} = 1$ (see next paragraph). Table 2 lists the standard values of the Lorentz factor of the jets, the dependence of the specific TDE rate on SMBH mass, the fraction of the intrinsic jet luminosity in $L_{\rm X}$, and the upper mass boundary of tidally disrupted stars. The index of the redshift evolution is assumed to be either $p = 0$ (no evolution case) or 4 (strong

Table 2. Default Setting of Fixed Parameters

$\lambda_{\rm Edd}$	Γ	λ	$\eta_{\rm jet}$	$M_{*,\rm max}$
[1]	[2]	[3]	[4]	[5]
1.0	10	-0.4	0.1	1.0

Notes.
Col. [1]: Eddington ratio. Col. [2]: The Lorentz factor. Col. [3]: Index for the $M_{\rm BH}$ dependence of the TDE rate. Col. [4]: Fraction of the intrinsic luminosity of the jet in $L_{\rm X}$. Col. [5]: Upper mass boundary of disrupted stars in units of solar mass.

Table 3. Best-fit parameters

p	$f_{\rm jet}$	$\psi_0\xi_0$	p-value ($L_{\rm X}^{\rm obs}$-dist/z-dist)
[1]	[2]	[3]	[4]
0	$0.012^{+0.122}_{-0.010}$	$1.7^{+1.6}_{-0.9}$	0.16/0.14
4	$0.003^{+0.027}_{-0.002}$	$1.6^{+1.6}_{-0.9}$	0.60/0.40

Notes.
Col. [1]: Index of the redshift evolution. Col. [2]: Fraction of the TDEs with jets. Col. [3]: Normalization factor of XLF in units of 10^{-8} Mpc^{-3} $\log L_{\rm X}^{-1}$ yr^{-1}. Col. [4]: p-value on the basis of the KS-test for each parameter of $L_{\rm X}^{\rm obs}$ and z.

evolution case). According to the prediction of numerical simulations that the occurrence rate of TDEs increases with the star-formation rate (Aharon et al. 2016), the latter case simply assumes that the TDE rate is proportional to the star-formation rate density, which evolves with $\propto (1+z)^4$ (Pérez-González et al. 2005). Eventually, only $\phi_0\xi_0$ and $f_{\rm jet}$ are left as free parameters.

We calculate the likelihood function over a redshift range of $z = 0$–1.5. The luminosity range is derived from the SMBH range of $\log(M_{\rm BH}/M_\odot) = 4$–8 for a given $\lambda_{\rm Edd}$ (1.0). To convert the mass into the X-ray luminosity $L_{\rm X}$, we consider $\lambda_{\rm Edd} = 1.0$ and a spectra described in Section 3.1. (the blackbody, Comptonization, and jet components). Specifically, we first determine the ratio of the Comptonized component in the 2–10 keV band to the bolometric luminosity without the jet component. Assuming that accretion physics in TDEs is similar to that of AGNs, we refer to the results by Vasudevan & Fabian (2007), who derived the bolometric correction factor ($k_{2\text{-}10}$) from the 2–10 keV band to be $\sim$50 for $\lambda_{\rm Edd} = 1.0$. We then convert the luminosity in the 2–10 keV band to that in the 4–10 keV band by assuming a power-law photon index of 2.0. As a result, $\log L_{\rm X}$ spans a range from 40.2 to 44.2 for $\lambda_{\rm Edd} = 1.0$. The integration range of M_* is determined to satisfy the criterion $R_{\rm TDE}/R_{\rm Sch} \geq 1$.

Table 3 summarizes the results of the ML fit for the cosmological evolution index of $p = 0$ and $p = 4$. The results are acceptable in terms of the KS-test at 90% confidence level. The $f_{\rm jet}$ upper and lower limits, where the $\mathcal{L}$-value is increased by 2.7 from its minimum, are derived. Since the ML method cannot directly determine the normalization ($\psi_0\xi_0$) of the luminosity function, we calculate it so that the predicted number from the model equals to the detected number of the TDEs. The attached error corresponds to the Poisson error in the observed number at the 90% confidence level based on equations (9) and (12) in Gehrels (1986).

Figure 2 displays the results of the TDE XLF as a function of $L_{\rm X}^{\rm obs}$ (observed peak luminosity in the 4–10 keV band), obtained for the case of $p = 4$. The solid curves plot the best-fit model at $z = 0.75$, which is obtained by integrating $\mathrm{d}\Phi(L_{\rm X}, z = 0.75)/\mathrm{d}L_{\rm X}$ over the half solid angle with respect to the jet direction, the mass of disrupted stars, and $L_{\rm X}$ (intrinsic peak luminosity of the Comptonized component) as

$$\begin{aligned}&\Pi(\log L_{\rm X}^{\rm obs}, z = 0.75)\\ &= \ln(10)\ L_{\rm X}^{\rm obs} \int\int\int \mathrm{d}L_{\rm X}\mathrm{d}\log M_* \frac{\mathrm{d}\Omega}{2\pi}\\ &\times\Big\{(1-f_{\rm jet})\delta_{\rm D}(C_0 L_{\rm X} - L_{\rm X}^{\rm obs}) + f_{\rm jet}\delta_{\rm D}\Big(C_1 L_{\rm X} - L_{\rm X}^{\rm obs}\Big)\Big\}\\ &\times\frac{\mathrm{d}\Phi(L_{\rm X}, z = 0.75)}{\mathrm{d}L_{\rm X}} P(M_*). \qquad (11)\end{aligned}$$

The data points are plotted by the "$N^{\rm obj}/N^{\rm model}$" method (Miyaji et al. 2001). The error bars reflecting the 90% confidence level of $N^{\rm obj}$ are derived based on Gehrels (1986).

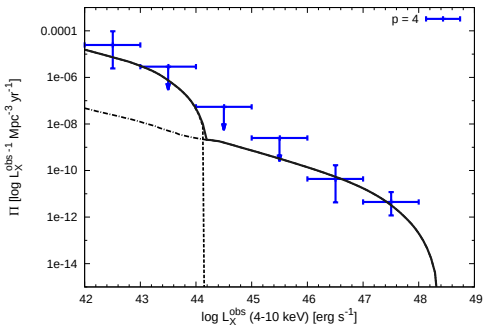

Fig. 2. The best-fit XLF as a function of "observed" peak luminosity at $z = 0.75$ for an evolution index of $p = 4$. The solid line represents the total XLF consisting of that of TDEs without jets (dotted line) and that of TDEs with jets (dot-dashed line).

3.6. Mass Accretion History of SMBHs by TDEs

TDEs contribute to the growth of SMBHs as argued by Soltan (1982) for AGNs. We here calculate the evolution of the mass density of SMBHs by TDEs as done for AGNs. The bolometric luminosity of a TDE can be related to the mass accretion rate $\dot{M}_{\rm acc}$ via the mass-to-radiation conversion efficiency ϵ as

$$L_{\rm bol} = \epsilon c^2 \dot{M}_{\rm acc}. \qquad (12)$$

The mass growth rate of the SMBH is given by

$$\dot{M}_{\rm BH} = (1-\epsilon)\dot{M}_{\rm acc}. \quad (13)$$

We formulate the SMBH mass-density equation as

$$\rho(z) = \int_{z_{\rm s}}^{z} {\rm d}z \frac{{\rm d}t}{{\rm d}z} \int_{L_{\rm X,min}}^{L_{\rm X,max}} {\rm d}L_{\rm X} \frac{{\rm d}\Phi(L_{\rm X},z)}{{\rm d}L_{\rm X}} \int_{M_{*,\rm min}}^{M_{*,\rm max}} P(M_*) {\rm d}\log M_* \times \frac{1-\epsilon}{\epsilon c^2} \int_{t_{\rm p}}^{\infty} \{(1-f_{\rm jet})L_{\rm peak} + f_{\rm jet} L_{\rm peak}^{\rm jet}\} \left(\frac{t}{t_{\rm p}}\right)^{-5/3} {\rm d}t, \quad (14)$$

where $z_{\rm s}$, $L_{\rm peak}$, and $L_{\rm peak}^{\rm jet}$ are the initial redshift from which the calculation starts, the peak bolometric luminosity without jets, and that with jets. Here, $L_{\rm peak}$ is set to the Eddington luminosity, while $L_{\rm peak}^{\rm jet}$ is the sum of the Eddington luminosity and intrinsic jet luminosity. By adopting the mass-to-radiation conversion efficiency of $\epsilon = 0.1$ similarly to the case of AGNs, we calculate the cumulative SMBH mass-density ($M_\odot$ Mpc^{-3}) from $z_{\rm s} = 1.5$ for the case of $p = 4$. We find that the total mass density at $z = 0$ would become at most $7\times10^2 M_\odot$ Mpc^{-3} by TDEs only, with a very small increase ($3.8 \times 10^5 M_\odot$ Mpc^{-3}) from that at $z = 1.5$ (Figure 3). Figure 3 compares the cumulative SMBH mass-density by TDEs and that of AGNs estimated by Ueda et al. (2014), indicating that the mass-density contributed by TDEs is much less than that of AGNs.

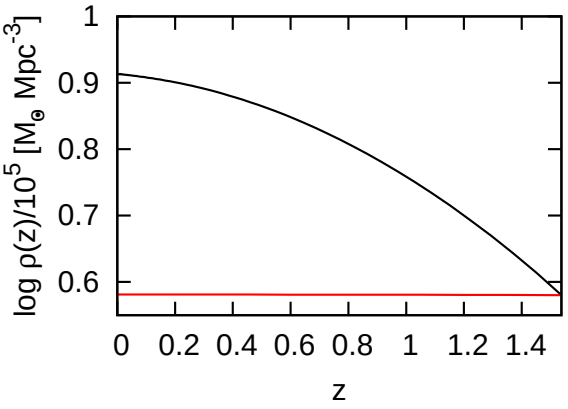

Fig. 3. The evolution of SMBH mass-density caused by TDEs (red) and AGNs (black).

4. Summary

We have derived the XLF of TDEs, i.e., the occurrence rate of a TDE per unit volume as a function of intrinsic peak luminosity, from the *MAXI* extragalactic survey. Our sample consists of four TDEs detected in the first 37 months *MAXI*/GSC data at high Galactic latitudes ($|b| > 10°$). It is complete to a flux limit of $\sim 3 \times 10^{-11}$ erg s^{-1} cm^{-2} (4–10 keV).

We formulate the shape of the TDE XLF, based on the mass function of SMBHs and the specific TDE rate as a function of SMBH mass. We take account of two distinct types of TDEs, those with jets and those without them, and also the relativistic beaming from the jets. To incorporate effects of the cosmological evolution, we assume two cases where the XLF is constant over redshift or is proportional to $(1+z)^4$. ML fits are performed to the observed TDE sample, with the normalization of the XLF (i.e., TDE rate) and the fraction of TDEs with jets among all TDEs, $f_{\rm jet}$, allowed to vary. Resultant $f_{\rm jet}$ is constrained to be 0.0007%–34%, consistent with the case of AGNs. Eventually, based on the XLFs, we find that the effect by TDEs to the growth of SMBHs is negligible at $z \lesssim 1.5$.

References

Aharon, D., Mastrobuono Battisti, A., & Perets, H. B. 2016, ApJ, 823, 137
Blanton, M. R., Dalcanton, J., Eisenstein, D., et al. 2001, AJ, 121, 2358
Brown, G. C., Levan, A. J., Stanway, E. R., et al. 2015, MNRAS, 452, 4297
Burrows, D. N., Kennea, J. A., Ghisellini, G., et al. 2011, Nature, 476, 421
Cenko, S. B., Krimm, H. A., Horesh, A., et al. 2012, ApJ, 753, 77
Donley, J. L., Brandt, W. N., Eracleous, M., & Boller, T. 2002, AJ, 124, 1308
Gehrels, N. 1986, ApJ, 303, 336
Hiroi, K., Ueda, Y., Hayashida, M., et al. 2013, ApJS, 207, 36
Kawamuro, T., Ueda, Y., Shidatsu, M., et al. 2016, PASJ, 68, 58
Komossa, S., & Bade, N. 1999, A&A, 343, 775
Kroupa, P. 2001, MNRAS, 322, 231
Magorrian, J., & Tremaine, S. 1999, MNRAS, 309, 447
Marconi, A., & Hunt, L. K. 2003, ApJ, 589, L21
Matsuoka, M., Kawasaki, K., Ueno, S., et al. 2009, PASJ, 61, 999
Mihara, T., Nakajima, M., Sugizaki, M., et al. 2011, PASJ, 63, 623
Milosavljević, M., Merritt, D., & Ho, L. C. 2006, ApJ, 652, 120
Miyaji, T., Hasinger, G., & Schmidt, M. 2001, A&A, 369, 49
Nikołajuk, M., & Walter, R. 2013, A&A, 552, A75
Pérez-González, P. G., Rieke, G. H., Egami, E., et al. 2005, ApJ, 630, 82
Phinney, E. S. 1989, The Center of the Galaxy, 136, 543
Soltan, A. 1982, MNRAS, 200, 115
Stone, N. C., & Metzger, B. D. 2014, arXiv:1410.7772
Sugizaki, M., Mihara, T., Serino, M., et al. 2011, PASJ, 63, 635
Ueda, Y., Akiyama, M., Hasinger, G., Miyaji, T., & Watson, M. G. 2014, ApJ, 786, 104
Vasudevan, R. V., & Fabian, A. C. 2007, MNRAS, 381, 1235